Role of the Antenna in Tissue Selective Probes Built of Lanthanide−Organic Chelates

B. Andes Hess, Jr.,*,† A. Kędziorski,‡ L. Smentek,†,‡ and D. J. Bornhop†

Department of Chemistry and Vanderbilt Institute of Chemical Biology, Vanderbilt University, Nashville, Tennessee 37325, and Institute of Physics, Nicolaus Copernicus University, Toruń, Poland

Received: July 21, 2007; In Final Form: December 3, 2007

The role of the antenna in the process of the host sensitized luminescence of the DOTA cage coordinated with the Eu ion is investigated. The analysis of the optimal geometries of DOTA modified by several antennas is based on the results of density functional theory (DFT) calculations. The physical environment of the luminescence center (the lanthanide ion) is illustrated by charge density maps and described by the values of the crystal field parameters directly evaluated. The conclusions derived from this theoretical analysis support earlier observations that antennas attached to the cage play the sole role of harvesting and transferring the energy to the lanthanide ion, whereas the cage perturbs the symmetry of the environment of the lanthanide ion, giving rise to the sensitized luminescence. The implications of the separation of the two parts of the organic chelate, cage and antenna, are discussed within the theoretical models of the energy transfer and of forced $f \leftrightarrow f$ electric dipole transitions.

1. Introduction

Dotarem [Gd-DOTA], *Magnevist* [Gd-DTPA], *Omniscan* [Gd-BMA-DTPA], and *ProHance* [Gd-HPDOTA] are contrast agents successfully used in clinical medicine to enhance NMR signals and to make the diagnosis of pathology in certain organs easier, or in some cases possible. However, there are recent reports on a possible causal correlation between the gadolinium-based contrast agents and development of a serious disease (known as Nephrogenic Systemic Fibrosis/Nephrogenic Fibrosing Dermopathy) in patients with kidney failure.[1] Such reports from practice very often ruin the beautiful picture of experiment and theory. At the same time a collision of the results of research with the realistic clinical applications, to which the research is originally addressed, is a very strong motivation for further investigations to learn how the agents work, in addition to the practical knowledge that they work.

From a physical point of view, the paramagnetic ion Gd is the best candidate from all the lanthanides to enhance nuclear magnetic resonance signals, because it possesses the highest magnetic moment resulting from its specific electronic structure of a half-filled shell of 4f symmetry. DOTA (1,4,7,10-tetraazacyclododecane-1,4,7,10-tetraacetic acid) and DTPA (dieethylenetriaminepentaacetic acid) in the names of the contrast agents above are examples of organic chelating ligands, which coordinate with the lanthanide ion. Organic chelates coordinated to other members of the lanthanide family are used to diagnose cancerous changes in various tissues.[2] The specific architecture of the cage depends on the kind of the tissue that absorbs the agent the most. In this case the interaction of the magnetic moments with the applied magnetic field is not the origin of the signal monitoring the cancer, but rather the luminescence of the lanthanide ions embedded in a particular environment. Because tumor cells absorb more of the agent than the healthy cells, the luminescence of lanthanides sensitized by the chelate has become a noninvasive and very sensitive tool for detecting abnormal changes at the level of a few molecules. The use of such tissue selective probes also makes it possible to treat the attacked tissues and destroy the tumors through local radiation when a radioactive lanthanide ion is used. There is also research on the possibility of attaching to the organic chelate a specific medicine to deliver it directly to the site. Such "dressing" of the chelate by chemotherapeutic agents might make it possible to replace standard chemotherapy, which is harmful not only for the cancer cells but also for the whole body, by a local treatment.

The results of experimental work performed on organic chelates coordinated with the lanthanide ions provide a plethora of information[3] about the architecture of cages, efficiency of the luminescence process, and correlation between the chemical structure of the agent and the specific tissues to which it is addressed. Unfortunately, theoretical investigations are very much behind the experimental knowledge, and still there are many unanswered questions awaiting reliable numerical analysis and constructive conclusions that may aid in finding new tools for diagnostic and therapeutic procedures.

To establish a reliable theoretical model of the spectroscopic properties of organic chelates coordinated to the lanthanide ions, a numerical analysis has been performed for derivatives of the organic chelate DOTA for which much is known from earlier experiments and theoretical investigations.[4−7]

2. Methodology

2.1. Model of Host Sensitized Luminescence. In general, the sensitized luminescence, observed as a signal, results from three consecutive steps, which are schematically represented in the Figure 1.

Although it is possible to excite the lanthanide ion directly with a powerful beam (which would be very harmful in clinical applications), normally, the cages are built to indirectly sensitize the luminescence. Therefore, in Figure 1 the organic chelate, pictured as a closed cage with the lanthanide ion placed inside,

* Corresponding author. E-mail: b.andes.hess@venderbilt.edu.
† Vanderbilt University.
‡ Nicolaus Copernicus University.

10.1021/jp075736y CCC: $40.75
Published on Web 02/26/2008

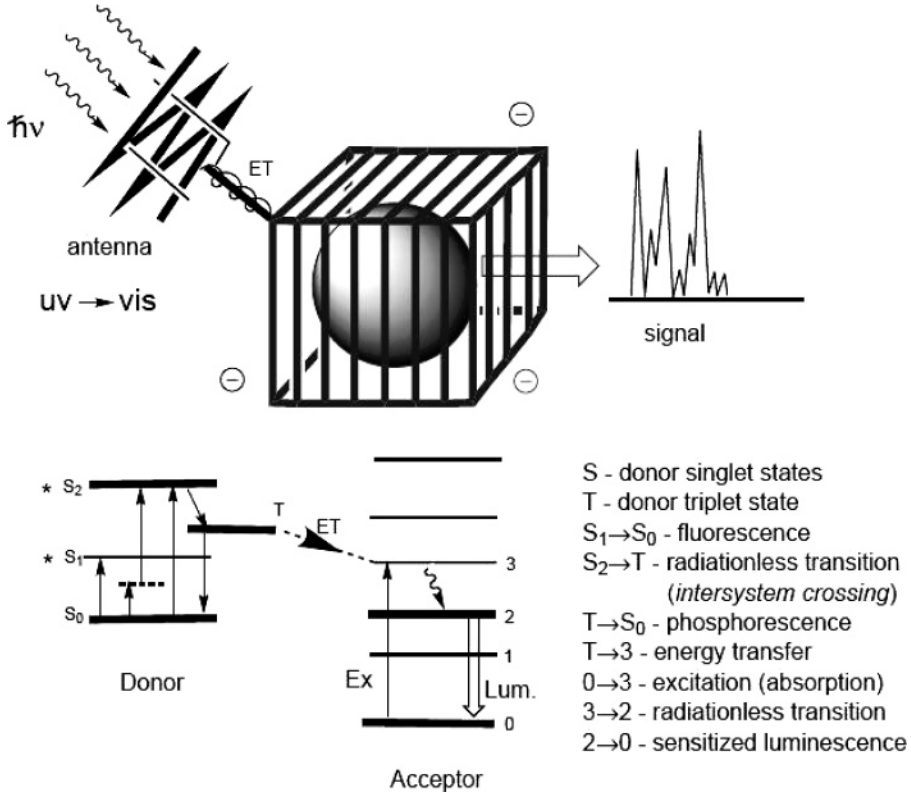

Figure 1. Scheme of the sensitized luminescence of the lanthanide ion coordinated with the cage of the organic chelating ligand; the Jabłoński diagram is presented below in the illustration.

is modified by an attached chromophore, which acts as an antenna and harvests the light. As illustrated in the Jabłoński diagram in Figure 1, there are indeed three steps in the process from which sensitized luminescence originates as the final signal:

1. harvesting the light from the external beam by a sensitizer, which results in excitation of the antenna from the ground singlet state to an excited singlet state, followed by a nonradiative transition (inter-system crossing), leading to a triplet state;

2. energy transfer from the donor in its triplet state to the acceptor, the lanthanide ion, which becomes the center of luminescence; due to spin selection rules this energy transfer occurs rather than radiation to the lower energy state of the antenna. Sensitization (excitation) of the lanthanide is thermodynamically favorable, if the energy of the antenna is greater that the excitation energy of the lanthanide ion. Therefore, often the lanthanide ion is excited to a very high energetic state, and the lower excited state, from which the luminescence is observed in the solution, is reached via nonradiative transitions;

3. luminescence of the lanthanide ion, which is observed as a signal characterized by very sharp atomic-like spectral lines.

Because the UV light is usually absorbed by the organic chelate with visible light being produced as a signal, the caged lanthanide plays the role of a light-converting device. However, there is an intensive search for compounds that absorb light in the visible region. The most desirable for in vivo applications are chelates coordinated with the lanthanides that luminesce in the near IR, because in such cases the energy of the excited states of the lanthanide ion is low enough to use a beam of visible light to excite the antenna. Furthermore infrared radiation is better for work with biological samples, because its penetration depth is much greater than in the case of visible light.

To be able to predict, design, and build effective and noninvasive diagnostic tools, theoretical studies are now directed toward understanding all the distinct steps of the process of sensitized luminescence illustrated in Figure 1, the results of which research are presented here.

2.2. Design of an Efficient Chelate. The scheme in Figure 1 demonstrates that certain conditions have to be satisfied to obtain a chelate with the required properties. To understand the physics of the sensitized luminescence of organic chelates coordinated with the lanthanide ions, extensive studies reported here were performed for several compounds. In particular, to analyze and establish the role of antennas in the cancer detecting signals, an analysis was performed for parent DOTA coordinated with the Eu ion along with its derivatives containing various antennas attached to the cage via different bridges.

The Eu ion is the most stable ion of the lanthanides and has more predictable properties than the other lanthanides. Its energy scheme is rather simple, and its spectroscopic properties are defined by specific selection rules resulting from the symmetry of the ground state, $^7F_0$. The first excited state, from which the luminescence is observed as a signal, is of ^5D_J symmetry. Among all possible electric dipole transitions between the ground and excited states, the transition between the levels $^5D_0 \leftrightarrow {}^7F_0$ is of greatest interest. This particular transition is used as a criterion for the identification of the structure of the compound and its symmetry. This is how it was verified that the DOTA chelate exists in two isomeric forms, because in the spectrum of the chelate coordinated with Eu two sharp lines resulting from the electric dipole transition $0 \leftrightarrow 0$ are observed.[4] This has been experimentally confirmed by the results of numerical calculations (density functional theory, DFT) for the DOTA chelate coordinated with all lanthanide ions.[7]

The structures taken into account in our analysis, for which the DFT calculations of the optimized geometry have been carried out, are presented in Figure 2. The abbreviations used for various chelates are the following: P_A, aniline attached to

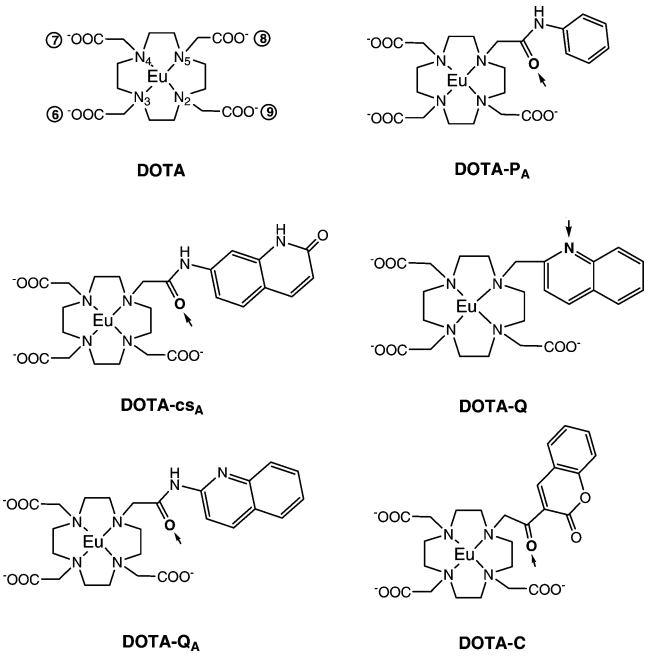

Figure 2. Schematic illustration of the organic chelates DOTA coordinated with Eu ion and modified by various antennas. The atom of the antenna, which coordinates with the Eu is designated by a small arrow.

the cage via the amide bridge; Q, quinoline attached to the cage via a methylene group; Q_A, quinoline attached via the amide bridge; C, coumarin; cs_A, carbostyril 124 attached via an amide bridge. The atoms indicated by an arrow in Figure 2 are those of the antennas, which are found to be coordinated with the central ion instead of the original acetate oxygen of the parent system. These investigations for DOTA were performed to satisfy the "design principles" summarized by T. Gunnlaugsson and J. P. Leonard in their review article:[8]

1. The hydration state of the environment of the lanthanide ion should be $q = 0$, where q is the number of coordinated water molecules, as defined by Parker; this condition leads to the maximum quantum yield, because possibly present water molecules quench the lanthanide luminescence.[9]

2. In accordance with the Dexter's electrostatic model of energy transfer, the attached antenna should be close to the lanthanide ion to maximize the efficiency of the sensitization.

3. The absorption of the antenna should be correlated with the excitation requirements of the caged lanthanide ion.

The ligands should encapsulate the lanthanide ion tightly to give a compact cage that is stable thermodynamically and kinetically. This condition is of especial importance for in vivo applications, because it limits the toxicity of the lanthanides by separating them from the biological environment.

The calculations of the optimal geometry of the analyzed complexes were carried out using the program GAUSSIAN 03.[10] All calculations were done with DFT (B3LYP functional) and utilized the 6-31G* basis set[11] for all atoms except for the lanthanides. For the lanthanide ions the quasi-relativistic effective core potential (ECP) of Dolg and the related (5s4p3d)-GTO valence basis sets were applied.[12] This means that for the tripositive lanthanides $46 + 4f^N$ electrons are included in the core, and the remaining electrons are treated explicitly. In all cases full geometry optimizations were performed and the resulting geometries were confirmed by the computation of the second derivatives of the energy to be minima on the potential surface (all positive eigenvalues of the Hessian).

2.3. Charge Density Maps. To study the actual changes in the vicinity of the lanthanide ion, charge density maps have been generated. These maps reflect the physical reality surrounding the lanthanide ion, which as a center of the luminescence, is sensitive to its environment. The charge density is defined in a standard way, namely

$$\rho(\vec{r}_i) \equiv \rho(\vec{r}_i,\vec{R}_1,...,\vec{R}_m) = N \sum_{\text{spin}} \int \mathrm{d}\vec{r}_1 ... \mathrm{d}\vec{r}_{i-1}\, \mathrm{d}\vec{r}_{i+1} ... \mathrm{d}\vec{r}_N\, |\Psi(x_1,...,x_N;\vec{R}_1,...,\vec{R}_m)|^2$$

where N is the number of electrons and m denotes the number of nuclei. The wave function depends on the coordinates of all electrons, $x_i \equiv \vec{r}_i\sigma$, and in a parametric way on the positions of all nuclei. In the maps presented below the step between two iso-charge lines is 0.025 au; the outermost external line corresponds to this initial value, and the charge density increases in the direction of the nuclei.

3. Results and Discussion

3.1. Optimal (DFT) Geometry. In Figure 3 optimized structures obtained for parent DOTA and five examples of the cage with the attached antennas P_A, cs_A, Q, C, and Q_A are presented.

In parent DOTA the organic chelate has a structure of a cage built of four nitrogen atoms (N_2, N_3, N_4, and N_5 in Figure 2), which form the basal plane, and of four oxygen atoms from the acetate arms that are coordinated with the lanthanide ion and form the capping plane that closes the cage (O_6, O_7, O_8, and O_9 in Figure 2). The definition of these planes is presented in Figure 4, in which a third plane that contains the lanthanide ion and which is parallel to the basal plane is also shown.

The parent system is of C_4 symmetry, which has been confirmed computationally.[6,7] When one of the acetate arms of the parent system is replaced by an antenna, the C_4 symmetry is obviously disturbed. The main goal of the present investigations is to verify to what extent this distortion occurs in each of the modified chelates, and what influence it has on the spectroscopic features of the compound.

As seen in Figure 3 for DOTA-P_A, the oxygen atom from the amide bridge linking the antenna to the main cage is the fourth atom of the capping plane, and it is coordinated with the lanthanide ion to close the cage. It replaces the oxygen atom of the original acetate arm of parent system. The antenna in DOTA-Q is attached to the cage directly, and the nitrogen atom from the quinoline was found to be coordinated to the central ion. As anticipated, it is seen that indeed the C_4 symmetry of the cage is disturbed by the incorporation of these antennas. However, at this point of analysis, the question remains unanswered whether this perturbation of the symmetry affects the physical environment of the lanthanide ion to the extent that the complex would display different spectroscopic properties.

When the quinoline antenna is attached to the cage via the amide bridge, as in DOTA-Q_A, instead of the nitrogen of the previous case, now the carbonyl oxygen atom of the amide bridge is coordinated to the central ion. Although the antenna is pushed away from the cage, the coordination sphere and vicinity of the lanthanide ion are more symmetrical than in the case of cage with the antenna attached directly. These observations are supported by detailed examination of the DFT structures. The distances of the coordinated atoms from the central ion for the optimal DFT geometry of each given in Figure 3 as well those of the other coordinated atoms (oxygen and

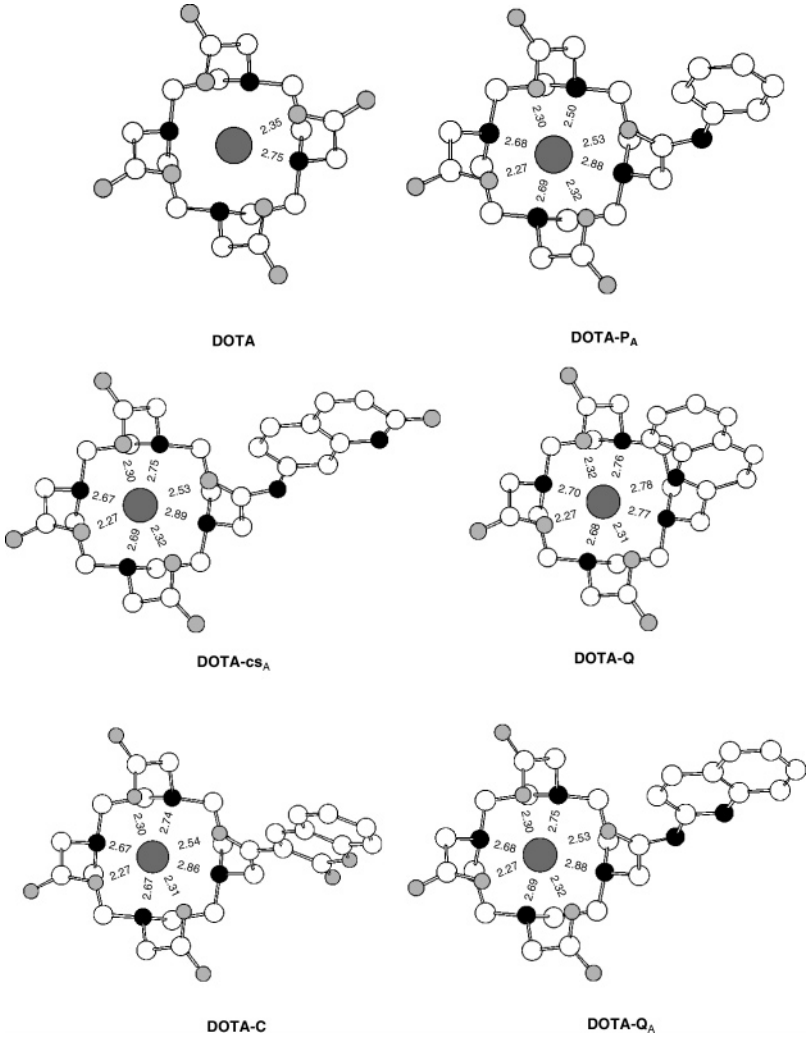

Figure 3. Optimal geometry of DOTA and DOTA modified by various antennas; results of numerical DFT calculations. Numbers (in Ångstroms) shown on the figures are the bond distances between oxygen and nitrogens atoms and the Eu^{+3} ion. Nitrogen atoms are black and oxygens are gray.

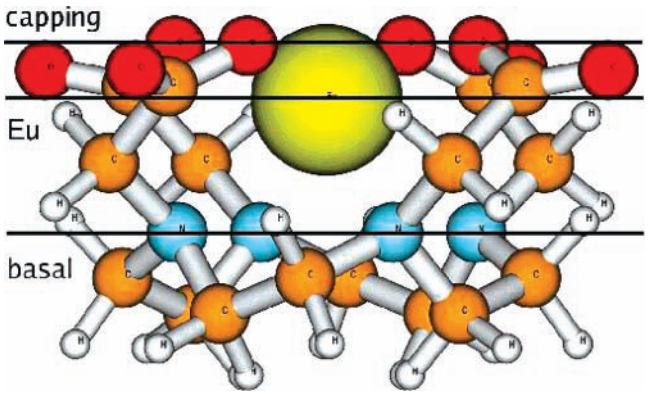

Figure 4. Definition of basal, Eu, and capping planes.

nitrogen). In all cases an oxygen atom of the antenna, (which belongs in most cases to the amide linkage) is coordinated, except for DOTA-Q, in which the fourth coordinated atom is nitrogen.

Inspection of the structures evaluated for the four complexes with their antennas attached via the amide linkage, and their comparison to those of the symmetric cage of parent DOTA, suggests that the antenna is not important in the description of the environment of the luminescence center (lanthanide ion). The average distances from the lanthanide ion of all nitrogen atoms, as well as all the oxygen atoms in DOTA-P_A, DOTA-cs_A, and DOTA-Q_A, are very close to their respective distances in the parent system. These are the chelates in which the antenna is attached via an amide bridge, and its oxygen atom completes the 8-fold coordination of the central ion. This conclusion is supported also by comparison of the results obtained for DOTA-Q_A and DOTA-Q. These two chelates differ only by the linkage of the same antenna to the cage (see Figures 2 and 3). As mentioned above, when the amide bridge is used, the antenna is moved away from the cage in comparison to its position when it is attached directly to the cage. These results demonstrate that the shape of the cage of DOTA-Q_A, as expected, is closer to that of the parent system, which is of C_4 symmetry. Therefore, the optimal geometry of DOTA-Q_A is more symmetrical than that of DOTA-Q. This means that it is possible to treat the eight coordinated atoms (four nitrogens from the basal plane and four oxygen atoms from the capping plane) as the most important and influential neighborhood of the lanthanide ion. As a consequence, the physical situation in all these complexes, DOTA, DOTA-P_A, DOTA-cs_A, DOTA-C, and DOTA-Q_A, as *seen* or *felt* by the lanthanide ion, is almost the same. This conclusion provides strong theoretical support for Li and Selvin's suggestion,[13] based on spectroscopic evidence obtained by them for several cases, that antennas connected to the cage by the amide bridge have the carbonyl oxygen coordinated to the lanthanide ion. The computational results presented here also support their suggestion that the environment of the

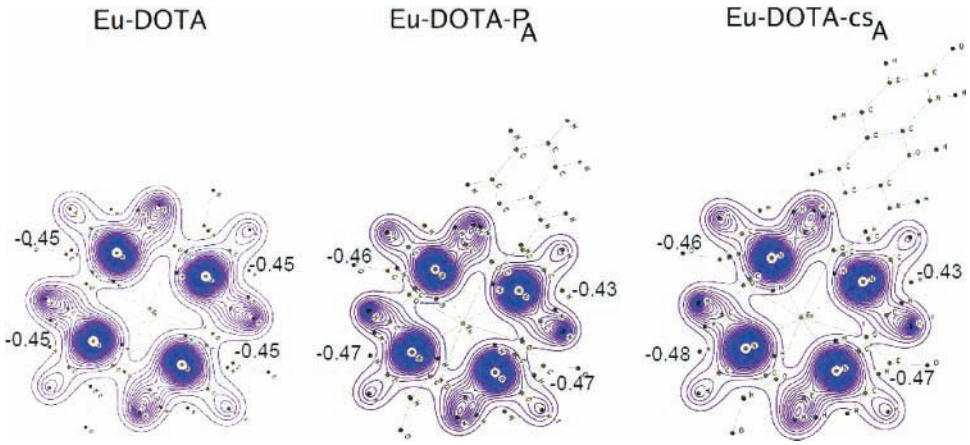

Figure 5. Charge density maps at the basal plane of parent DOTA, and two examples of the parent complex modified by an antenna, DOTA-P_A and DOTA-cs_A. The values presented in the figure are the Mulliken charges (in au) for the coordinated nitrogen atoms.

lanthanide chelated to DOTA with an antenna linked via an amide bridge is not greatly perturbed from that of the parent DOTA (without the antenna). In fact, it is not surprising that the oxygen of the amide linkage mimics the negative charge of the oxygen of the carboxylate anion so well. Indeed, it has long been known that the high stability of the amide functional group results from a significant contribution of the resonance structure in which there is a negative charge on the oxygen atom:

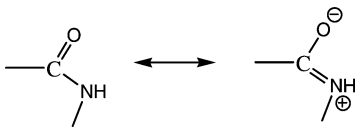

In the chelate, contributions from this type of resonance structure involve not separation of charge as in the amide functional group by itself, but rather delocalization of the positive charge of the central europium ion.

This significant preservation of the C_4 symmetry also explains the observation that for several complexes the luminescence spectra are almost independent of the kind of attached antenna. The conclusion reached from the results of our calculations require further analysis to confirm their validity by means of the standard crystal field theory, which is presented below.

When such an analysis is performed, however, keeping in mind the requirements that must be met to build an efficient diagnostic agent, a dilemma has to be solved. The question is whether to construct agents with the symmetry of the parent system preserved as much as possible (at least in the vicinity of the luminescent center) and attach the antenna via the amide bridge as in the case of DOTA-Q_A or connect the antenna directly to the cage as in the case of DOTA-Q, which results in moving the antenna closer to the lanthanide ion, but at the same time causing a distortion of the symmetry of parent system. The problem of symmetry or asymmetry (or rather disturbed symmetry) of the organic chelates modified by various antennas is one of the points that stimulated the present investigations.

3.2. Charge Density Maps. The charge density maps are generated along three planes, which are defined in Figure 4: the basal plane, the plane in which Eu is placed (which is parallel to the basal plane), and the capping plane. In the last case, when the fourth coordinated atom of the capping plane comes from the connecting bridge or directly from the antenna, the capping plane, is distorted by tenths of a degree from the planar arrangement. This is why in all such cases the capping plane is defined by the three oxygen atoms from the remaining three original acetate arms of the parent system.

The optimal DFT geometries of the analyzed systems suggest that in all cases the modifications of the structure of the parent system are not large, if the antenna replaces one of the acetate arms. As seen from Figure 3, the most stable part of the cage, almost independent of the attached antenna, is the basal plane, which is determined by the four nitrogen atoms coordinated with the lanthanide ion (see the distances between the central ion and the black circles, which in Figure 3 represent the nitrogen atoms). This stability of the base of the cage is very well illustrated in the maps presented in Figure 5.

The maps in Figure 5 reflect the physical situation on the basal planes of three different cages: parent DOTA (for comparison), DOTA-P_A, and DOTA-cs_A. In all these cases the large maxima correspond to the four nitrogen atoms. Other local maxima are produced by the hydrogen atoms, which are out of the basal plane, but close enough to contribute to the map of the charge density. The central ion is above the basal plane and therefore is not visible in these maps. As anticipated from the discussion of the optimal geometries of the chelates, it is seen also from this figure that the distribution of the charge density is practically the same in all these cases. The values of Mulliken charges (in au) localized on the nitrogen atoms from the basal plane are also presented in the Figure 5. It is seen that these charges in the case of derivatives of the Eu-DOTA complex are only slightly changed from those for the parent system and are practically the same for all systems. Thus, it is justified to conclude that, to a good approximation, the C_4 symmetry of the basal plane is preserved when the antennas are attached. In fact, it should be pointed out that the atoms of both antennas are far from the basal plane (both are attached via the amide bridge, which provides the oxygen atom to complete the coordination with the lanthanide ion), and they indeed do not contribute to the physical conditions at the level of basal plane.

The lanthanide ion contributes to the charge density at the level of its position in the cage. This situation is shown in Figure 6, where the charge density maps obtained for the Eu-plane of DOTA-P_A and DOTA-cs_A are compared with the map for parent DOTA. The central maximum in each map corresponds to the position of the Eu ion in the cage. It is interesting to note that there is some accumulation of charge density along the directions between the central ion and the coordinated oxygen atoms. This particular part of the map is rather characteristic of the distortion of the spherical cloud, and it corresponds to the shift of some amount of the charge from the oxygens toward the central ion. This electrostatic interaction is responsible for the stability of

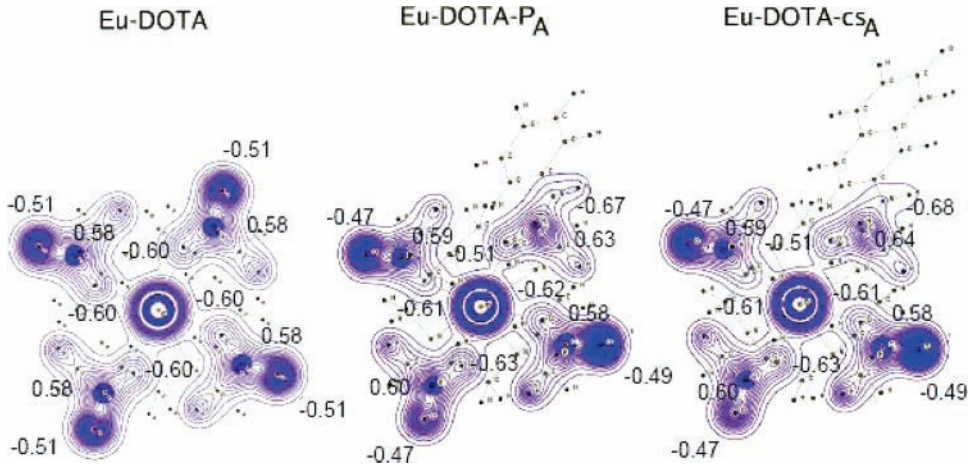

Figure 6. Charge density maps taken from the plane of the Eu ion. The values presented in the figure are the Mulliken charges (in au). The four numbers in the center of each map correspond to the four coordinated oxygen atoms. The next four values from the center correspond to the oxygen atoms of the carboxyl groups except in the case of DOTA-P_A and DOTA-cs_A, where one of these Mulliken charges (the closest to the antenna) arises from the nitrogen of the amide bridge. The four outermost values correspond to the four carbon atoms of the carbonyl groups.

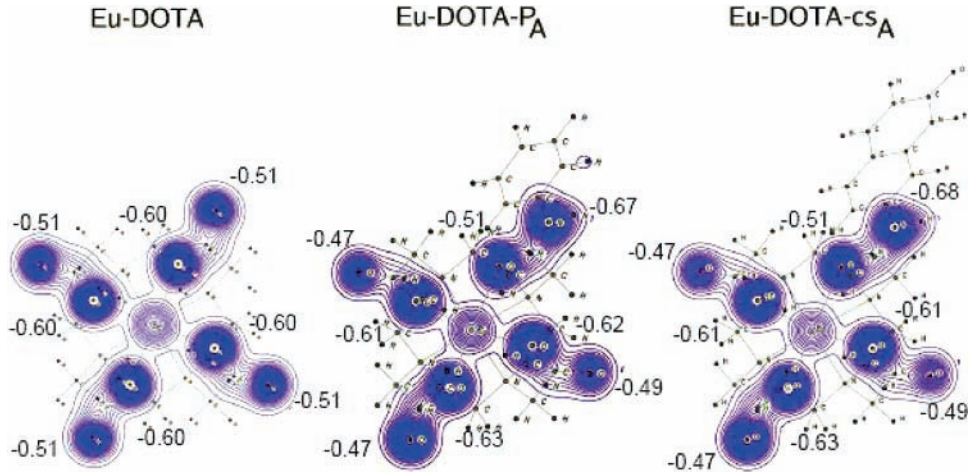

Figure 7. Charge density maps for the capping planes. The values presented in the figure are the Mulliken charges (in au). The four inner values on the map correspond to the four coordinated oxygen atoms. The outer values on each map correspond to oxygen atoms from carboxyl groups; in the case of DOTA-P_A and DOTA-cs_A the value near to antenna is the Mulliken charge for nitrogen from amide bridge.

the system and also plays the role of a physical mechanism, which is the origin of the spectroscopic properties of these systems.

The innermost sets of four numbers are the Mulliken charges that are calculated for the coordinated oxygen atoms of the four arms. These four oxygen atoms in all three cases lie in the capping plane and hence are barely visible in Figure 6. In the case of the parent system, all of these coordinated oxygens arise from carboxyl groups. For the two derivatives (with antennas) one of these coordinated oxygens is part of the amide group, as indicated in Figure 3. The next set away from the central ion are Mulliken charges that arise from the uncoordinated oxygen atoms of the arms (carbonyl oxygens), except for the arms which incorporate the antennas in which case they arise from the nitrogen of the amide group. Finally the outermost set of Mulliken charges arise from the carbons of the carboxylate and amide groups.

It is seen from Figure 6 that first of all the charge distribution is essentially independent of the antenna, because almost the same maps are obtained for P_A and cs_A. This result again supports the observation that the luminescence spectra of a given lanthanide ion is almost the same when the various antennas are attached to the main cage of the organic chelate. Does it mean that the crystal field and its perturbing influence upon the lanthanide ion (responsible for the $f \leftrightarrow f$ electric dipole transitions) is the same in all these cases? Although these charge density maps provide some insight into the understanding of the propertiaues of chelates, some additional crystal field analysis is still required to derive reliable conclusions. This is why the physical environment of the central ion illustrated in Figure 6 is analyzed below in terms of the crystal field theory.

The charge density maps obtained for the capping planes (Figure 7) show again that the closest environment of the luminescence center is almost the same in all cases. The origin of the values of the Mulliken charge densities is clearly presented in Figure 7 where the charge clouds close up the vicinity of the central ion from above.

It is seen from Figure 7 that the central ion enters the capping plane, because there is a charge accumulation in the center of each map. It is interesting to analyze the maps for the cages with antennas, while remembering that the fourth coordinated atom (oxygen) comes from the amide bridge; these are the maxima closest to the central one, and their Mulliken charges (in au) are shown by the four inner values on each map. The more distant maxima originate from the noncoordinated oxygen atoms of the carboxyl arms (three) and from the nitrogen atom (not coordinated) of the amide bridge; their Mulliken charges are given by the outer values on each map. Only the structures

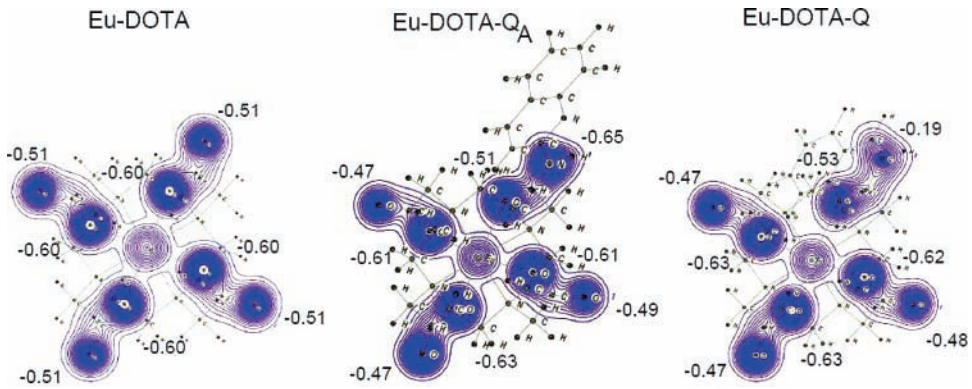

Figure 8. Charge density maps for the capping planes. The values presented in the figure are the Mulliken charges (in au). The four inner values on the maps for DOTA and DOTA-Q_A correspond to four coordinated oxygen atoms, and for DOTA-Q the fourth charge density originates from the coordinated nitrogen atom of Q. The outer values on each map correspond to oxygen atoms from carboxyl groups; in the case of DOTA-Q_A and DOTA-Q the value near to antenna is the Mulliken charge for nitrogen from amide bridge and carbon from quinoline, respectively.

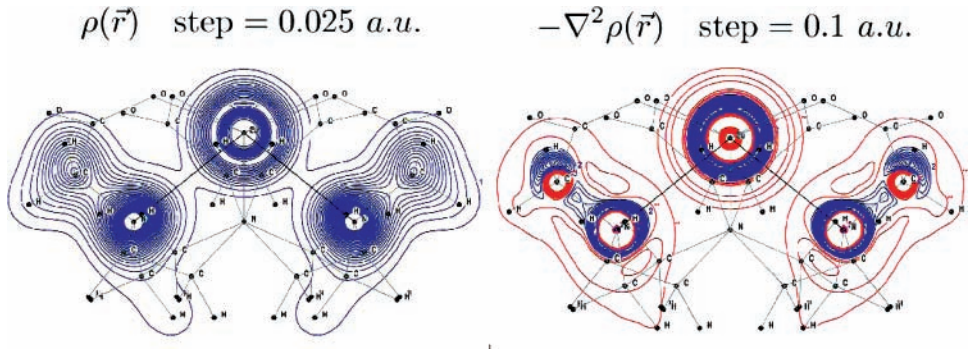

Figure 9. Charge density map and the map of $\nabla^2\rho$ for parent DOTA taken along the vertical slice (two nitrogen atoms and C_4 axis).

of the compounds drawn in the background of these maps show the differences between these figures, because the maps are almost the same as that for the parent system (where all four oxygen atoms come from the carboxyl arms).

As illustrated in Figure 7, the values of atomic charges for the coordinated oxygens of the acetate arms slightly decrease (it is a larger negative charge) in the Eu-DOTA derivatives in comparison to the corresponding values for parent system; this means that electronic charge for these atoms increases. The opposite situation is in the case of the coordinated oxygen atom from the amide bridge, for which the electronic charge density diminishes. Finally, it is seen that the corresponding Mulliken charges for DOTA-P_A and DOTA-cs_A are practically the same.

It is interesting to compare the charge distribution for the DOTA cage with the quinoline antenna attached via the amide bridge (more compact chelate), DOTA-Q_A, and when it is attached directly (via CH_2), DOTA-Q. The situation is illustrated in Figure 8 where the charge density maps taken from the capping plane, as an example, are compared to that of DOTA. Even without a detailed analysis of numerical results it is seen that the physical reality represented by the charge densities in the case of DOTA-Q_A is very close to that in the parent DOTA. As a consequence, to a good approximation DOTA-Q_A may be treated as having axial symmetry. This means that in these two cases, DOTA and DOTA-Q_A, the lanthanide ion *feel*s the potential, although of different physical origin, but of the same symmetry. In the case of DOTA-Q (map at the right-hand side of Figure 8) the situation is different, and there is a perturbation around the charge, which is localized on the carbon atom of quinoline; in this case the symmetry of the lanthanide environment is disturbed. This observation is confirmed by inspection of the Mulliken charges presented (in au) in the Figure 8. It is seen that the trends of changes of the values of the Mulliken charges are the same as in the case of the situation presented in Figure 7. In addition, it is interesting to note that the Mulliken charges for the appropriate atoms of the Eu-DOTA-Q_A complex are practically the same as those for Eu-DOTA-P_A and Eu-DOTA-cs_A complexes illustrated in Figure 7.

The change of the environment of the central ion in the Eu-DOTA-Q complex is manifested by different values of the Mulliken charges in comparison to their counterparts from the systems, where the antenna is attached to the cage via an amide bridge. The results of this analysis lead to the very important conclusion that a crucial role in the perturbing influence of the environment upon the lanthanide ion is played by the linkage of an antenna to the cage.

The above conclusions, which are derived from the analysis of the charge density maps, make the search for the answer to the question about the role of antenna in the whole process of the sensitized luminescence of the lanthanide ion even more urgent. To find additional information about the environment of the central ion, it is possible to analyze the charge density distribution as a function of many coordinates trying to find its minima and maxima using standard analytical geometry. This is the reason that the Laplacian of the charge density has been investigated. As an example, in Figure 9, the cage sliced by the plane containing two nitrogen atoms of the basal plane and the C_4 axis (vertical slice) is presented in terms of the charge density map and the map of the negative values of the Laplacian of charge density. If the latter are positive, they indicate the local accumulation (concentration) of the charge density, and they are drawn as blue lines; the negative values mean a local depletion of the charge density, and they are drawn in red.

From all the charge density maps presented here it is evident that there is coordination between the lanthanide ion and the four nitrogen atoms and four oxygen atoms (like in the DOTA

TABLE 1: Values of the Structural Parameters B_p^t (in 10^{-4} au) for DOTA, DOTA-P_A, DOTA-cs_A, DOTA-Q_A, and DOTA-Q

B_p^t		DOTA		DOTA-P_A		DOTA-cs_A		DOTA-Q_A		DOTA-Q	
t	p[a]	Re	Im	Re	Im	Re	Im	Re	Im	Re	Im
1	0	2.64		5.35		5.13		5.66		−29.33	
	1			−40.48	−56.31	−41.57	−59.57	−41.63	−55.88	−64.29	−51.17
2	0	−52.84		−45.78		−44.56		−45.11		−50.53	
	1			−2.29	−3.98	−2.28	−4.35	−2.00	−4.05	−9.90	−8.47
	2			5.27	−8.50	5.45	−8.48	5.37	−8.48	−0.99	−14.21
3	0	−14.05		−14.04		−14.05		−14.05		−12.88	
	1			0.70	−0.51	0.63	−0.60	0.73	−0.57	−0.18	0.48
	2			0.44	−2.98	0.46	−3.09	0.42	−2.99	−0.24	−3.35
	3			7.29	−2.81	7.57	−2.87	7.45	−2.74	6.38	−3.59
4	0	−2.10		−2.67		−2.80		−2.77		−2.66	
5	0	1.28		1.28		1.27		1.27		−1.23	
6	0	0.13		0.16		0.16		0.16		0.16	

[a] $(B_p^t)^* = (-1)^p B_{-p}^t$.

parent system), but not a chemical bond, which could be understood in a standard way as "sharing" the electrons by bonded atoms. This coordination rather than the chemical bonding is also seen in Figure 9, especially in its right-hand part, where $\nabla^2\rho$ is pictured. Indeed, in the space between the Eu ion and the neighboring nitrogen atoms there is a region with positive values of the Laplacian, which means that there is a relative depletion of the charge density. This picture demonstrates that *coordination* (chelating) holds the atoms of the cage and the lanthanide ion together rather than a chemical bond.

3.3. Crystal Field Analysis. The charge density maps generated for various planes of the organic chelates provide data for the crystal field potential in which the lanthanide ion is embedded. From a physical point of view this potential is responsible for the energy transfer and the process of luminescence. Although we realize how crude the model of a crystal field based on the point charge approximation is, to gather additional information about the cages and various antennas attached to them, some preliminary calculations have been performed. Due to the lack of a reliable model for the direct evaluation of the crystal field parameters, our attempts undertaken here are not a step backward but should be understood as the only practical possibility for the description of the environment of the lanthanide ion in a complex in terms of a physical quantity. To further justify this step of numerical analysis, it should be pointed out that all the complexes analyzed here are very similar to each other, and therefore, it may be expected that in the numerical calculations performed in a uniform way for all systems, at least the same errors are made by scaling the results. This means that not quantitative but rather qualitative conclusions are derived from the obtained results.

Using the charge densities illustrated here in all the maps, the crystal field potential was generated for the optimized DFT geometry of each system by applying the point charges localized on the atoms obtained from the Mulliken population analysis. Thus, the evaluated crystal field potentials should reflect the differences and similarities between the derivatives of Eu-DOTA complex that are observed in the analysis of the optimized geometry and charge density distribution presented in the maps. As mentioned, these calculations have been performed not to evaluate directly the impact of the crystal field upon the lanthanide ion but only to verify through the comparison of the results which differences, in a physical sense, are introduced by various antennas attached to the parent DOTA.

For future numerical analysis of the efficiency of the energy transfer between the antenna and the lanthanide ion, and also of the yield of the luminescence, it is crucial to establish a theoretical method for the evaluation of the crystal field parameters. In the best possible scenario, which is the availability of the energy levels of the lanthanide ion in the cage obtained from the assignment of spectroscopic lines and measurements, only the even rank crystal field parameters may be determined from the fitting procedure. This procedure has been used in a very interesting paper by Kang et al.,[14] where the even rank crystal field parameters have been determined for Eu-DOTA (parent system) and Eu-TETA (1,4,8,11-tetrazacyclotetradecane-1,4,8,11 tetraacetate). Unfortunately, the authors of this paper ignored the helical structure of the arms of parent DOTA and, as a consequence, performed the fitting procedure with the assumption that the cage is of C_{2v} symmetry, instead of C_4. Therefore, it is impossible to compare the results of their calculations with the values of even rank crystal field parameters evaluated and presented here. It would be ideal to also perform similar experiments for the chelates modified by various antennas. To our knowledge, however, there are no such results yet reported in the literature, and therefore, the numerical analysis has to be limited to the results of direct calculations, as presented here.

As mentioned, a fitting procedure[14] is the best source of the crystal field parameters of even ranks. However, to evaluate directly the amplitudes of energy transfer and the $f \leftrightarrow f$ transitions, the odd rank crystal field parameters are required. Because the latter do not contribute to the energy, they cannot be determined through the fitting procedure and, therefore, have to be evaluated directly. In fact, in the case of the intensities of the $f \leftrightarrow f$ transitions the intensity parameters might be determined via the semiempirical procedure based on Judd−Ofelt theory[15,16] or the relativistic parametrization scheme,[17] if the data of spectroscopic measurements are rich enough. Although this procedure would reproduce the observations of the intensities, it would not provide any insight into the origin of the spectroscopic properties of the chelates. Only *ab initio* type calculations are a reliable source of information that would allow one to better understand the physical conditions necessary for obtaining efficient signals. This issue is especially important in the case of understanding energy transfer, which initiates the luminescence process, because still so little is known and understood about its physical reality.

In Table 1 the values of the structural parameters evaluated within the point charge model approximation for DOTA, DOTA-P_A, DOTA-cs_A, DOTA-Q_A, and DOTA-Q are collected (for simplicity of presentation, for the parameters with the rank $t = 4, 5, 6$ only the values for the components $p = 0$ are included). These are simply the values of the crystal sums, which are determined by the angular parts and radial term R^{-t}, for $t =$

TABLE 2: Structural Parameters B_p^t (in 10^{-4} au) for DOTA-P_A Divided into Components Resulting from Various Groups of Atoms

				bridge							
B_p^t		cage		coord. atom		rest		antenna		total	
t	p^a	Re	Im	Re	Im	Re	Im	Re	Im	Re	Im
1	0	−34.89		65.82		−5.52		−20.07		5.3	
2	0	−38.72		−17.52		10.06		0.40		−45.78	
3	0	−11.02		−3.71		0.49		0.20		−14.04	
4	0	−2.66		0.18		−0.20		0.02		−2.67	
	4	−2.93	−1.78	−0.69	−0.58	−0.02	0.19	0.01	0.00	−3.63	−2.17
5	0	1.15		0.15		−0.02		0.00		1.28	
	4	−1.30	−0.48	−0.13	−0.11	−0.01	0.01	0.00	0.00	−1.43	−0.57
6	0	0.14		0.01		0.00		0.00		0.16	
	4	0.05	−0.03	0.00	0.00	0.00	0.00	0.00	0.00	0.06	−0.03
7	0	−0.04		0.01		0.00		0.00		−0.04	
	4	0.02	0.02	0.00	0.00	0.00	0.00	0.00	0.00	−0.03	0.02

[a] $(B_p^t)^* = (-1)^p B_{-p}^t$.

1, 2, ..., 7, where R is the distance of the point charges localized on various atoms from the central ion. Due to this radial dependence, the structural parameters for lower ranks are more sensitive to the distances, and consequently, to the geometry of the cage. Thus it is expected that the changes of the geometry of the parent system resulting from the replacement of one acetate arm by an antenna are reflected more strongly by values of the lower rank parameters. Indeed, it is seen from Table 1 that the most sensitive are the values of crystal field parameters for $t = 1$, whereas for $t \geq 3$ their values are almost the same for all systems.

The results in Table 1 provide numerical support for the conclusions derived from the graphical representation of the charge densities presented above in the form of the maps. Thus it is possible to conclude that the lanthanide ion placed inside the cages DOTA-P_A, DOTA-cs_A, and DOTA-Q_A (in all three cases the antennas are attached via the amide bridge) feels essentially the same influence of the physical environment (crystal field potential) as for the parent DOTA; in terms of the values of the charge densities localized on various atoms the situation is indeed illustrated in Figures 5−7. The situation is different in the case of DOTA-Q for which the discrepancy between the appropriate parameters in comparison to those for the other complexes is rather large (see the results displayed in Figure 8). The tendency of changes in the values of the structural factors for various ranks is also different from the previous cases. It is interesting to recall again that the quinoline antenna in DOTA-Q is attached directly to the cage, and the coordination of the nitrogen ion with Eu makes the whole chelate more compact, because the antenna is bent toward the central ion.

The results collected in the last two columns of Table 1 are the numerical representation of the differences observed between the charge density maps for DOTA-Q_A and DOTA-Q in Figure 8. It is seen especially from the last column of this Table that indeed the distortion of the geometry of the parent complex (as presented in Figure 3 and on the maps of the charge distributions) is reflected by the values of the crystal field parameters; in this particular derivative of DOTA the central ion is embedded in a crystal field potential, which is different from the potential in the other systems.

The general conclusion derived from the analysis of results collected in Table 1 shows that, even for lower ranks, the crystal field parameters are rather independent of the kind of attached antenna. Indeed, the values of crystal field parameters for DOTA-P_A, DOTA-cs_A, and DOTA-Q_A are almost the same in spite of the fact that the antennas are different; note that in all these cases the antennas are attached via the amide bridge. In the light of this conclusion it would be interesting to analyze distinct contributions to the values of crystal field parameters that originate from three separate groups of atoms. Namely, the crystal sums are divided into components caused by the main cage (parent DOTA without one arm), bridge and antenna. As an example, the results of such an analysis performed for DOTA-P_A are presented in Table 2.

It is striking when inspecting the values collected in Table 2 that for all cases except for $t = 1$, there are no contributions originating from the antenna. A similar distribution of various contributions to the crystal sums is also observed for the other complexes in which the antenna is attached via the amide bridge.

Thus, this is additional evidence that the antenna does not contribute to the crystal field potential surrounding the lanthanide ion, but rather it plays the sole role of harvesting of the energy, its transfer, and sensitization of the luminescence. This conclusion, although requiring more numerical verification, allows one to separate various parts of the chelate and assign to them distinct roles in the luminescence process, as presented in Figure 1. At the same time, this approximation simplifies the theoretical description of the energy transfer and the $f \leftrightarrow f$ transitions, which are the actual signals monitoring the presence of cancerous cells.

Some additional comments regarding the crystal field parameters for $t = 1$ are required. The observed sensitivity of these parameters to the environment can be understood, because of all the parameters they depend the strongest on the distance of the ligand from the origin. However the fact that $B_0^1 = 5.35$ for DOTA-P_A and 5.13 for DOTA-cs_A demonstrates that, regardless of the kind of antenna, the lanthanide ion feels almost the same crystal field potential in both systems. However, from the comparison of these values with 2.64 for parent DOTA, it is possible to determine that the geometry of the original cage is distorted (rather slightly, as seen in Figure 3) when the antenna is attached. Following this trend of thought one should remember that not the numerical values, but rather the relative magnitude of these parameters evaluated within the point charge model are important. It is also interesting to recall that the crystal field parameters with $t = 1$ are those which determine the amplitude of the $f \leftrightarrow f$ hypersensitive transitions. This means that, already at this point of theoretical investigations devoted to the optimal geometry of the chelates, it is possible to foresee the source of problems with the description and reproduction of the hypersensitive electric dipole transitions known from the literature.

4. Conclusions

The analysis presented here starts with the optimal geometry evaluated by means of the DFT model for the parent DOTA system and its modification by various antennas. The results of these calculations have been transformed into the physical quantity of charge density, the distributions of which are presented graphically by maps generated at various slices of the analyzed complexes. Using the simple concept of crystal sums, the maps have been translated into the numerical values of the crystal field parameters that define the crystal field potential influencing the lanthanide ion; this potential is the physical origin of spectroscopic properties of the chelates. As the title of this paper indicates, the main aim of performed investigations was to establish the role of the antenna in the process of the host-sensitized luminescence illustrated schematically in the Figure 1.

The main conclusion derived as a result of present analysis is that the antenna attached to the cage does not perturb the physical environment of the lanthanide ion when compared to that of the parent system. In spite of the fact that the attached antenna disturbs the global symmetry of the chelate, in practice the immediate environment of the lanthanide ion is not changed and still is of C_4 symmetry. This is especially the case when an amide linkage is used to tether the antenna to the cage, as in DOTA-P_A, DOTA-CS_A, and DOTA-Q_A. In light of the numerical results presented here it is a good approximation to regard the neighborhood of the lanthanide ion as limited to the coordinated atoms. This partitioning of the complex and assignment to the antenna the sole role of harvesting the energy and sensitizing the luminescence have serious implications, which lead to a simplification of the theoretical model of energy transfer and $f \leftrightarrow f$ transitions as presented in the Appendix.

Acknowledgment. The support of the National Science Foundation (Bes-0323281) and the National Institutes of Health (P20 GM072048-02) is acknowledged.

Appendix

It is standard procedure to describe the energy transfer between the sensitizer and activator by Dexter's expression,[18]

$$\rho_{s\rightarrow A} = \frac{T_6}{R^6} + \frac{T_8}{R^8} + \frac{T_{10}}{R^{10}} + ... \quad (1)$$

where R is the distance between both centers and T_6, T_8, and T_{10} are the terms associated with the dipole−dipole, dipole−quadrupole, and quadrupole−quadrupole interactions, respectively. These terms are usually treated as parameters. In direct calculations they are determined by appropriate matrix elements of the electric dipole, electric quadrupole, and higher multipole radiation operators between the functions describing the energy states of activator and sensitizer.

Taking into account the electrostatic interactions between the rare earth ion (RE) and ligands (L), the amplitude of the energy transfer is determined by the matrix element,[19−22]

$$\left\langle \Psi_{RE}(1)\,\Phi_L(2)\left|\sum_k \frac{r_<^k}{r_>^{k+1}}(C^{(k)}\cdot C^{(k)})\right|\Psi'_{RE}(1)\,\Phi'_L(2)\right\rangle \quad (2)$$

where the distinct functions are localized on two different centers, and therefore, the matrix element above is usually separated into the product of two elements evaluated separately for the central ion and the ligand. When the multipole expansion is applied for the Coulomb interactions between both subsystems, the matrix element has the following form

$$\langle f|V|i\rangle = \sum_{m\mu}\sum_{kq}[k,m,k+m]^{1/2}(4\pi)^{-3/2}\frac{C_{-q-\mu}^{(k+m)}(\Theta\Phi)}{R^{k+m+1}} \times B_{km}^{q\mu}\langle 4f^N\Psi_f|D_q^{(k)}|4f^N\Psi_i\rangle\langle\Phi_f^L|D_\mu^{(m)}|\Phi_i^L\rangle \quad (3)$$

where k and m denote the ranks of the multipoles $D^{(k)}$ and $D^{(m)}$ localized on the lanthanide ion and ligand, respectively. The angular factor, together with the radial dependence on the distance between the centers, describes the geometry of the chelate. The matrix elements in eq 3 contribute to the parameters T of Dexter's simple expression. The distances in particular powers in the denominators of eq 1 are evaluated from the general expression (3) (squared because the matrix elements in eq 3 define the energy transfer amplitude, not the intensity) for $k = m = 1$ (dipole−dipole interactions), for $k = 1$, $m = 2$, and $k = 2$, $m = 1$ (dipole−quadrupole interactions and *vice versa*), and finally for $k = m = 2$ (quadrupole−quadrupole interactions) (the higher order multipoles are neglected in eq 1). The wave functions $4f^N\Psi_f$ and $4f^N\Psi_i$ describe in the best way possible the final and initial states of the lanthanide ion prior to the luminescence and after it. Using the achievements of theoretical model of the electric dipole $f \leftrightarrow f$ transitions developed previously,[15,16] it is straightforward to deduce that to describe the energy states of the lanthanide ion in a chelate, of all possible physical mechanisms, first the corrections due to the perturbing influence of the surrounding crystal field have to be taken into account. This procedure requires the knowledge of the crystal field parameters; for even rank multipoles, the even rank crystal field parameters are required, and for the odd rank multipoles, the odd rank crystal field parameters are required. Thus the question remains how to evaluate the crystal field parameters. The task is dramatically simplified if the crystal field in the chelates is indeed created only by the cage limited to the coordinated atoms, as concluded above.

The simplification due to the separation of the antenna from the main cage is even more beneficial in the case of a direct evaluation of the second matrix element in eq 3. In general, the functions Φ_i^L and Φ_f^L describe the energy states of the ligands before and after energy transfer. Again, if the antenna is responsible only for the harvesting of the energy and transferring it to the luminescence center, these functions in practice describe the energy states of antenna and not the whole organic chelate. This is a major simplification, which makes practical *ab initio* type calculations possible. The separation of the antenna from the cage is even more important in the case of evaluation of the contributions to the energy transfer amplitude originating from the exchange interactions, which requires the evaluation of two center integrals.[23]

These conclusions, and resulting from them simplifications of the theoretical model, define very well a starting point for further analysis of efficiency of the energy transfer and host sensitized luminescence of lanthanide coordinated organic chelates.

Note Added in Proof. Aita, Temma, Kuge and Saji have reported (*Luminescence*, **2007**, *22*, 455) the synthesis of a DOTA modified by fluorescein as an antenna attached to the cage by an amide bridge as discussed here. This macrocycle when coordinated with Nd(III) is a candidate for in vivo applications, since the infrared luminescence is sensitized by visible light.

References and Notes

(1) Private communication, M. Ayad, Vanderbilt University Medical Center.

(2) Storr, T.; Thompson, K. H.; Orvig, C. *Chem. Soc. Rev.* **2006**, *35*, 534.

(3) *Reviews in Flurorescence 2005*; Geddes, C. D., Lakowicz, J. R., Eds.; Springer: Berlin, 2005.

(4) (a) Kang, S. I.; Ranganathan, R. S.; Emswiller, J. E.; Kumar, K.; Gougou, J. Z. tas; Tweedle, M. F. *Inorg. Chem.* **1993**, *32*, 2912. (b) Kumar, K.; Chang, C. A.; Francesconi, L. C.; Dischino, D. D.; Malley, M. F.; Gougoutas, J. Z.; Tweedle, M. F. *Inorg. Chem.* **1994**, *33*, 3567. (c) Hoeft, S.; Roth, K. *Chem. Ber*. **1993**, *126*, 869. (d) Aime, S.; Botta, M.; Fasano, M.; Marques, M. P. M.; Geraldes, C. F. G. C.; Pubanz, D.; Merbach, A. E. *Inorg. Chem*. **1997**, *36*, 2059. (e) Jacques, V.; Desreux, J. F. *Inorg. Chem.* **1994**, *33*, 4048. (f) Brittain, G. H.; Desreux, J. F. *Inorg. Chem.* **1984**, *23*, 4459.

(5) (a) Eisenstein, O.; Maron, L. *J. Organomet. Chem*. **2002**, *647*, 190. (b) Boehme, C.; Coupez, B.; Wipff, G. J. *J. Phys. Chem. A* **2002**, *106*, 6487. (c) Luo, Y.; Selvam, P.; Koyama, M.; Kubo, M.; Miyamoto, A. *Chem. Lett*. **2004**, *33*, 780. (d) Miguirditchian, M.; Guillaneaux, D.; Guillaumont, D.; Moisy, P.; Madic, C.; Jensen, M. P.; Nash, K. L. *Inorg. Chem*. **2005**, *44*, 1404. (e) González-Lorenzo, M.; Plastas-Iglesias, C.; Avecilla, F.; Faulkner, S.; Pope, S. J. A.; de Blas, A.; Rodriguez-Blas, T. *Inorg. Chem*. **2005**, *44*, 4254. (f) Gutierrez, F.; Rabbe, C.; Poteau, R.; Daudey, J. P. *J. Phys. Che*m. *A* **2005**, *109*, 4325. (g) Henriques, E. S.; Bastos, M.; G. C. Geraldes, C. F.; Ramos, M. J. *Int. J. Quantum Chem*. **1999**, *73*, 237. (h) Keire, D. A.; Jang, Y. H.; Li, L.; Dasgupta, S.; Goddard, W. A., III; Shively, J. E. *Inorg. Chem*. **2001**, *40*, 4310. (i) Di Vaira, M.; Stoppioni, P. *New J. Chem.* **2002**, *26*, 136. (j) Moreau, J.; Guillon, E.; Aplincourt, P.; Pierrard, J.; Rimbault, J.; Port, M.; Aplincourt, M. *Eur. J. Inorg. Chem.* **2003**, *2003*, 3007.

(6) (a)Cosentino, U.; Moro, G.; Pitea, D.; Villa, A.; Fantucci, P. C.; Maiocchi, A.; Uggeri, F. *J. Phys. Chem. A* **1998**, *102*, 4606. (b) Cosentino, U.; Villa, A.; Pitea, D.; Moro, G.; Barone, V.; Maiocchi, A. *J. Am. Chem. Soc*. **2002**, *124*, 4901.

(7) Smentek, L.; Hess, B. A., Jr.; Cross, J. P.; Manning, H. C.; Bornhop, D. J. *J. Chem. Phys.* **2005**, *123*, 244302.

(8) Gunnlaugsson, T.; Leonard, J. P. *Chem. Commun*. **2005**, 3114.

(9) Parker, D.; Dickins, R. S.; Puschmann, H.; Cossland, C.; Howard, J. A. K. *Chem. Rev.* **2002**, *102*, 1977.

(10) Frisch, M. J.; Trucks, G. W.; Schlegel H. B.; et al., *GAUSSIAN 03*; Gaussian, Inc.: Pittsburgh, PA, 2003.

(11) Basis-set descriptions may be found in the work of: Foresman, J. B.; Frisch, A. E. *Explorin*g *Chemistr*y *wit*h *Electronic Structur*e *Methods*, 2nd ed.; Gaussian Inc.: Pittsburgh, PA, 1996.

(12) Dolg, M.; Stoll, H.; Savin, A.; Preuss, H. *Theor. Chim. Acta* **1989**, *75*, 173.

(13) Li, M.; Selvin, P. R. *J. Am. Chem. Soc*. **1995**, *117*, 8132.

(14) Kang, J.-G.; Na, M.-K.; Yoon, A.-K.; Sohn, Y.; Kim, Y.-D.; Suh, I.-H. *Inorg. Chim. Acta* **2000**, *310*, 56.

(15) Judd, B. R. *Phys. Rev*. **1962**, *127*, 750−761.

(16) Ofelt, G. S. *J. Chem. Phys*. **1962**, *37*, 511−520.

(17) Smentek, L. *J. Alloys Compd.* **2004**, *380*, 89.

(18) (a) Dexter, D. L. *J. Chem. Phys*. **1953**, *21*, 836. (b) Dexter, D. L. *Phys. Rev*. **1975**, *108*, 630. (c) Dexter, D. L. *Phys. Rev*. **1962**, *126*, 1962.

(19) Smentek, L.; Hess, B. A., Jr. *J. Alloys Compd.* **2000**, *300−301*, 165.

(20) Smentek, L.; Hess, B. A, Jr. *J. Alloys Compd.* **2000**, *315*, 1.

(21) Smentek, L.; Hess, B. A., Jr. *J. Alloys Compd.* **2002**, *336*, 56.

(22) Smentek, L.; Wybourne, B. G.; Hess, B. A., Jr. *J. Alloys Compd.* **2002**, *341*, 67.

(23) Smentek, L. *Int. J. Quantum Chem*. **2002**, *90*, 1206.